# Modeling and Construction of a Furuta Pendulum Prototype

**M. Antonio-Cruz**
**R. Silva-Ortigoza**
**C. A. Merlo-Zapata**
**M. G. Villarreal-Cervantes**
*Instituto Politécnico Nacional*
*CIDETEC. Área de Mecatrónica*
*Unidad Profesional Adolfo López Mateos*
*CP 07700, México, DF, Mexico*

**D. Muñoz-Carrillo**
*CINVESTAV-IPN*
*Departamento de Control Automático*
*CP 07360, México, DF, Mexico*

**V. M. Hernández-Guzmán**
*Universidad Autónoma de Querétaro*
*Facultad de Ingeniería*
*CP 76150, Querétaro, Qro, Mexico*

***Abstract*—In order to provide a material that can facilitate the modeling and construction of a Furuta pendulum, this paper presents the deduction, step-by-step, of a Furuta pendulum mathematical model by using the Lagrange equations of motion. Later, a mechanical design of the Furuta pendulum is carried out via the software SolidWorks and subsequently a prototype is built. Numerical simulations of the Furuta pendulum model are performed via Matlab-Simulink. Furthermore, the Furuta pendulum prototype built is experimentally tested by using Matlab-Simulink, ControlDesk, and a DS1104 board from dSPACE.**

***Keywords*-Mechatronics; Underactuated system; Furuta Pendulum; Prototype; Modeling; Mechanical design; Construction.**

## I. Introduction

The Furuta Pendulum, also known as rotary inverted pendulum, is a mechanism that has two degrees of freedom (DOF) and two rotational joints. It is essentially integrated by three elements: a motor and two bars called *arm* and *pendulum*. The motor's shaft is connected to one end of the *arm*, which causes the *arm* to be moved angularly in the horizontal plane, whereas the *pendulum* is joined to the free end of the *arm* through a link that can move freely and allows the rotation of the *pendulum* in the vertical plane. This mechanism is a popular device that has been used both as benchmark for the analysis of nonlinear control and for educational purposes (see, for example [1]–[8]). The main reasons of that are the simplicity and certain analogies with more complex systems, such as synchronous generators connected to an infinite bus and flight control systems, offered by the Furuta pendulum [9].

Literature associated with the modeling and construction of the Furuta pendulum is as follows. Regarding the modeling, in 2010, Acosta [10] described a quasi-conservative dynamic model, derived from the classical mechanics, which allows designing all the controllers as if the system was conservative. Other work provided by Cazzolato and Prime [11], in 2011, introduces a dynamics of the Furuta pendulum considering a full inertia tensor. That dynamics was derived by using two methods: a Lagrangian formulation and an iterative Newton-Euler formulation. More recently, in 2013, Jadlovská and Sarnovský [12] presented an application of a general procedure to derive a mathematical model of the rotary inverted pendulum with an arbitrary number of pendulum links. To design such a model Lagrangian equations and a Rayleigh dissipation function were used. The validity and accuracy of the mathematical model generated by the application were verified via numerical simulations. As regards the construction, in 2009, Allotta *et al.* [13] constructed two prototypes of the Furuta pendulum with the intention of providing test-beds for the laboratories of mechatronics, and complex dynamics and systems control of the University of Florence. In addition, the dynamic parameter identification of the real prototypes was carried out. In the study of García-Alarcón *et al.* [14], presented in 2012, a procedure to achieve the parameter identification of an experimental system associated with the Furuta pendulum, a computer aided design, and the system built were shown. Also, in order to validate such a procedure, results from numerical simulations of the system dynamic model were compared with experimental results from the system built.

Based on the literature review, it was found that few works have been exclusively dedicated to the modeling and construction of a Furuta pendulum. In such works, neither the mathematical model nor the construction of the system under study are described step-by-step. The latter could be of great help, since to implement or validate control laws in real time, the modeling and construction of a Furuta pendulum prototype are required. Thus, in order to contribute in this direction, this paper presents the modeling and construction in detail of a prototype associated with the Furuta pendulum, including the corresponding experimental verification.

The remaining of the paper is structured as follows. Section II deals with the deduction of the Furuta pendulum mathematical model; whereas, the design and construction of the system under study is treated in Section III. The numerical simulations of the Furuta pendulum model and the experimental tests of the prototype built are shown in

978-1-4673-6756-1/14 $31.00 © 2014 IEEE
DOI 10.1109/ICMEAE.2014.23

Section IV. Lastly, the conclusion is given in Section V.

## II. Modeling of the Furuta pendulum

In this section the deduction of the mathematical model of the Furuta pendulum is described in detail.

A graphical representation of the Furuta pendulum is shown in Figure 1. There, $\theta_0$ is the *arm* angular position measured with respect to an arbitrary position, $\theta_1$ is the *pendulum* angular position measured with respect to the upright position, $\tau$ is the torque (applied to the *arm*) generated by the electric motor, $I_0$ is the *arm* inertia (when it turns around one of its ends) and the motor inertia, $L_0$ is the *arm* length, $m_1$, $l_1$, and $J_1$ are the mass, the center of mass location, and the *pendulum* inertia, respectively. Lastly, $g = 9.81\ \mathrm{m/s^2}$ represents the gravity acceleration.

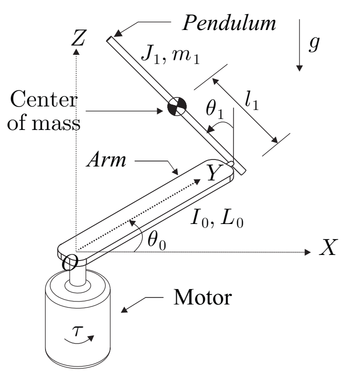


Figure 1. Furuta pendulum.

As the Furuta pendulum is a two DOF system, its dynamic model is given by two Lagrange equations of motion, which are defined by

$$\frac{d}{dt}\left(\frac{\partial L}{\partial \dot{\theta}_0}\right) - \frac{\partial L}{\partial \theta_0} = \tau, \tag{1}$$

$$\frac{d}{dt}\left(\frac{\partial L}{\partial \dot{\theta}_1}\right) - \frac{\partial L}{\partial \theta_1} = 0, \tag{2}$$

where $\dot{\theta}_0$ is the *arm* angular velocity, $\dot{\theta}_1$ the *pendulum* angular velocity, and $L$ the system Lagrangian determined as

$$L = K - V, \tag{3}$$

being $K$ and $V$ the kinetic energy and potential energy, respectively, of the Furuta pendulum system.

On the one hand, $K$ is the sum of the kinetic energy of the *arm* and the *pendulum*, which are, respectively, defined as follows:

$$K_0 = \frac{1}{2} I_0 \dot{\theta}_0^2, \tag{4}$$

$$K_1 = \frac{1}{2} J_1 \dot{\theta}_1^2 + \frac{1}{2} m_1 \upsilon_1^T \upsilon_1, \tag{5}$$

where $\upsilon_1$ is the linear velocity of the *pendulum* center of mass. Hence, an analysis of the Furuta pendulum kinematics is required. Then, from Figure 2, the location of the *pendulum* center of mass is determined by

$$x = [x_x,\ x_y,\ x_z]^T, \tag{6}$$

where $x_x$, $x_y$, and $x_z$ are defined as follows:

$$\begin{aligned}
x_x &= L_0 cos(\theta_0) - l_1 sin(\theta_1) sin(\theta_0), \\
x_y &= L_0 sin(\theta_0) + l_1 sin(\theta_1) cos(\theta_0), \\
x_z &= l_1 cos(\theta_1).
\end{aligned}$$

Thus, $\upsilon_1$ is given by

$$\upsilon_1 = [\dot{x}_x,\ \dot{x}_y,\ \dot{x}_z]^T, \tag{7}$$

being

$$\begin{aligned}
\dot{x}_x &= -\dot{\theta}_0 L_0 sin(\theta_0) - l_1 \Big(\dot{\theta}_0 sin(\theta_1) cos(\theta_0) + \\
&\quad + \dot{\theta}_1 sin(\theta_0) cos(\theta_1)\Big), \\
\dot{x}_y &= \dot{\theta}_0 L_0 cos(\theta_0) + l_1 \Big(\dot{\theta}_1 cos(\theta_0) cos(\theta_1) - \\
&\quad - \dot{\theta}_0 sin(\theta_0) sin(\theta_1)\Big), \\
\dot{x}_z &= -\dot{\theta}_1 l_1 sin(\theta_1).
\end{aligned}$$

After replacing (7) in (5) and reducing the resulting expression, the following is found:

$$\begin{aligned}
K_1 &= \frac{1}{2} J_1 \dot{\theta}_1^2 + \frac{1}{2} m_1 \Big[\Big(\dot{\theta}_0 L_0\Big)^2 + \Big(l_1 \dot{\theta}_0 sin(\theta_1)\Big)^2 + \\
&\quad + \Big(l_1 \dot{\theta}_1\Big)^2 + 2\dot{\theta}_0 \dot{\theta}_1 L_0 l_1 cos(\theta_1)\Big].
\end{aligned}$$

Therefore, the Furuta pendulum kinetic energy $K$ is given by

$$\begin{aligned}
K &= K_0 + K_1, \\
&= \frac{1}{2} I_0 \dot{\theta}_0^2 + \frac{1}{2} J_1 \dot{\theta}_1^2 + \frac{1}{2} m_1 \Big[\Big(\dot{\theta}_0 L_0\Big)^2 + \\
&\quad + \Big(l_1 \dot{\theta}_0 sin(\theta_1)\Big)^2 + \Big(l_1 \dot{\theta}_1\Big)^2 + \\
&\quad + 2\dot{\theta}_0 \dot{\theta}_1 L_0 l_1 cos(\theta_1)\Big].
\end{aligned} \tag{8}$$

On the other hand, $V$ is the sum of the potential energy of the *arm* and *pendulum*. Since the *arm* is moved on the horizontal plane, its potential energy is constant and can be considered equal to zero. Hence, the Furuta pendulum potential energy $V$ is reduced to the *pendulum* potential energy, that is:

$$V = -h m_1 g = m_1 g l_1 (cos(\theta_1) - 1). \tag{9}$$

Then, from (3), which has associated to (8) and (9), and after carrying out the corresponding derivatives in the equations system (1), (2), the dynamics of the Furuta pendulum is found as follows:

$$\tau = \alpha\ddot{\theta}_0+\beta\dot{\theta}_0\dot{\theta}_1+\gamma\ddot{\theta}_1-\sigma\dot{\theta}_1^2, \quad (10)$$

$$0 = \gamma\ddot{\theta}_0+(m_1 l_1^2+J_1)\ddot{\theta}_1-\frac{1}{2}\beta\dot{\theta}_0^2-m_1 g l_1 sin\,(\theta_1)\,, \quad (11)$$

where $\ddot{\theta}_0$ is the *arm* angular acceleration, $\ddot{\theta}_1$ is the *pendulum* angular acceleration,

$$\alpha = I_0+m_1L_0^2+m_1l_1^2 sin^2\,(\theta_1)\,, \quad \gamma = m_1L_0l_1 cos\,(\theta_1)\,,$$
$$\beta = m_1l_1^2 sin(2\theta_1), \quad \sigma = m_1L_0l_1 sin\,(\theta_1)\,.$$

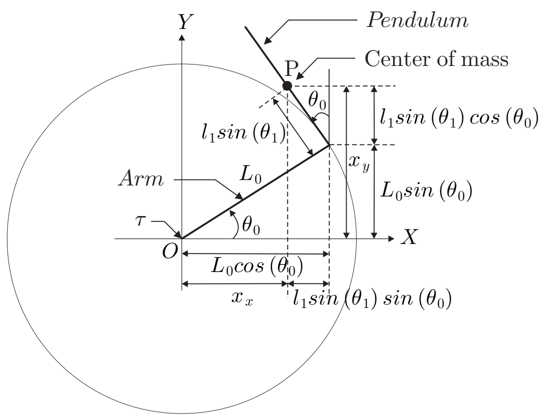


(a) Projection of the *arm* and *pendulum* in the horizontal plane.

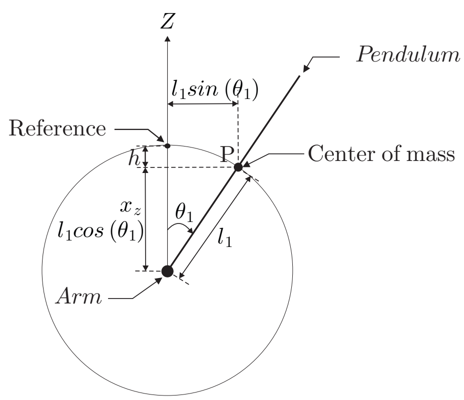


(b) Projection of the *pendulum* in the vertical plane.

Figure 2. Free body diagram of the system.

## III. Construction of the Prototype

The elements that integrate the Furuta pendulum prototype and the procedure followed in the construction of such a test-bed are presented below.

As shown in Figure 3, the Furuta pendulum prototype is composed –in general– of three blocks, namely: *subsystems*, *power stage*, and *data acquisition and processing*. The block *subsystems* refers to two subsystems, the first one corresponds to a DC permanent magnet motor and two encoders; whereas, the second is associated with a mechanical structure, that includes the mechanical elements that are, directly and indirectly, moved by the DC motor and those that hold the system. The block *power stage* is integrated by two power electronic devices, which as a whole provide energy to the DC motor. The block *data acquisition and processing* is associated with Matlab-Simulink, ControlDesk, and a DS1104 board from dSPACE, which allow the acquisition and processing of the data provided by the encoders.

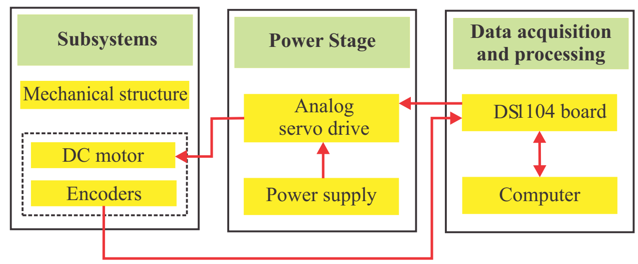


Figure 3. Block diagram of the prototype.

### A. Subsystems

This Section describes the subsystems integrated by a DC motor, two encoders, and a mechanical structure. The DC motor provides angular movement to the *arm*. The encoders are employed to sense the angular position of the *arm* and the *pendulum*. The mechanical structure was designed via the software SolidWorks, which is a tool for the mechanical design in 3D.

*1) DC motor and encoders:* Know the mechanical and electrical characteristics of the DC motor is not an easy task. Therefore, numerical simulations of the Furuta pendulum mathematical model were performed with the intention of determining the required torque to move the *pendulum* around its upright position (see Section IV). These simulations showed that the required torque is $0.17$ Nm. Thus, a 14204 Brush DC motor from Pittman was used.

Regarding the prototype encoders, two incremental encoders were used to obtain the angular position of the *arm* and *pendulum*. The encoder that allows sensing the *arm* position is included in the DC motor chassis and it has a $500$ CPR resolution; whereas, the encoder associated with the *pendulum* is an ITD 01 A 4 Y 1 optical mini encoder fabricated by Baumer with $1024$ CPR as maximum resolution.

*2) Mechanical structure:* The mechanical elements that compose the Furuta pendulum prototype were drawn and assembled, virtually, by using SolidWorks, since this software includes advanced functions that facilitate the part modeling, create assemblies, and generate plans easily and quickly. Also, SolidWorks allows specifying the material properties for each part of the Furuta pendulum prototype. Thus, a 3D model of such a prototype was generated as shown in Figure 4.

According to Figure 4, the description of each part that integrates the mechanical structure is as follows:

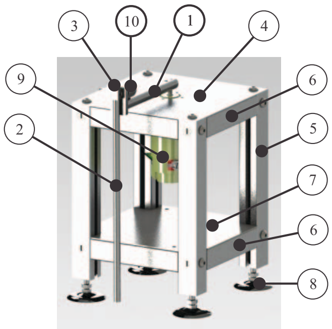


Figure 4. 3D model of the Furuta pendulum.

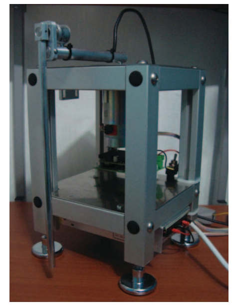

Figure 5. Furuta pendulum built.

① The *Arm* was manufactured from a T–6061 T–6 aluminum round bar with a $5/8''$ diameter.

② The *Pendulum* was made from a T–6061 aluminum tube with a $3/8''$ outer diameter and a T–6061 aluminum sheet. Furthermore, the *pendulum* includes the shaft that must be mounted into the *pendulum* encoder. The shaft was manufactured from a C–1018 round AISI with a $1/2''$ diameter.

③ The encoder holder is used to hold the encoder of the *pendulum*. This holder was made from a T–6061 aluminum sheet. This part includes a 628/6–2 z deep groove ball bearing from SKF.

④ The upper sheet is used to hold the DC motor with encoder and was manufactured from a stainless steel sheet.

⑤ The vertical aluminum profiles were made from Bosch tubular profiles. The weight of the remaining parts that compose the mechanical structure rests on such vertical profiles.

⑥ The horizontal aluminum profiles keep apart the vertical profiles to a certain distance, providing structural stability to the prototype.

⑦ The bottom sheet, manufactured on a stainless steel sheet, is used to hold the power supply that provides energy to the electrical and electronic devices.

⑧ The leveling legs are used to even the mechanical structure on a surface, which allows avoiding undesired movements of the prototype.

⑨ This part corresponds to the DC motor with encoder described in Section III-A1.

⑩ This part is associated with the *pendulum* encoder described in Section III-A1.

The prototype built can be seen in Figure 5.

It is important to mention that the mechanical design of the Furuta pendulum prototype was carried out in such a way that other configuration of pendulum can be set (see [15]).

### B. Power Stage

As was mentioned previously, the block *Power Stage* consists of two power electronic devices. The first one refers to a switched power supply of the HF100W–SF–24 model. This power supply provides energy to the DC motor, by means of the second power electronic device, that is, an analog servo drive, which is used to isolate the block *data acquisition and processing* from the DC motor. Also, this servo drive amplifies the current of a signal provided by the block *data acquisition and processing*, being the amplified signal the DC motor input signal. The servo drive is fabricated by Advanced Motion Controls in the model AZ12A8DDC. An important characteristic of such a servo driver is that it includes an internal control-loop, which avoids losses when the amplified signal is delivered to the DC motor.

### C. Data acquisition and processing

This Section describes the connection between the prototype and the DS1104 board from dSPACE. This board was selected due to the integration software between Matlab-Simulink and ControlDesk, that is, the board firmware.

In order to connect the prototype with the DS1104 board, a block diagram is programmed in the Matlab-Simulink environment. Such a program contains the blocks that generate the DC motor input signal and the blocks associated with the ports that the DS1104 board has to connect the incremental encoders and the analog servo drive. Once the encoders and the servo drive are connected to the DS1104 board, the program is executed by means of ControlDesk, which allows the acquisition and processing of the data provided by the encoders and by the DC motor input signal.

## IV. Simulations and experimental results

Numerical simulations associated with the model (10)-(11) and experiments obtained by using the prototype built of the Furuta pendulum are presented below.

### A. Results

In the implementation of the numerical simulations of the dynamics of the Furuta pendulum, that is, (10)-(11), the following values of the parameters were used:

$$I_0 = 0.4592 \text{ x } 10^{-3} \text{ Kgm}^2, \quad l_1 = 0.1475 \text{ m}$$
$$L_0 = 0.1414 \text{ m}, \qquad J_1 = 0.2755 \text{ x } 10^{-3} \text{ Kgm}^2,$$
$$m_1 = 0.038 \text{ Kg}.$$

Such values were obtained directly from the prototype built. The numerical simulations consisted in apply a constant torque to the *arm* during a period of time equal to 0.2 s, moving it from an arbitrary position, achieving that the *pendulum* reaches a position between $\pm 1$ rad around the upright position from its natural equilibrium point, that is, $\pm\pi$ rad. As regards to the experimental tests similar conditions to those used in the simulations were considered.

Both simulations and experimental tests were carried out in open-loop. The numerical simulations were performed by using Matlab-Simulink and the experimental tests were carried out via Matlab-Simulink, ControlDesk, and a DS1104 board.

The simulation results are shown in Figure 6, also this figure includes the experimental results obtained from the prototype built. With the purpose of differentiating the simulation results from the experimental ones, the following nomenclature was used. For the simulation results the variables $\theta_0$ and $\theta_1$, associated with the Furuta pendulum model (10)-(11), are denoted as $\theta_{0s}$ and $\theta_{1s}$, respectively. Likewise, $\theta_{0e}$ and $\theta_{1e}$ denote the experimental results of the same variables. The input of the system, $\tau$, is denoted as $\tau_s$ for the case of the simulations, whereas for the experimental results is defined as $\tau_e$.

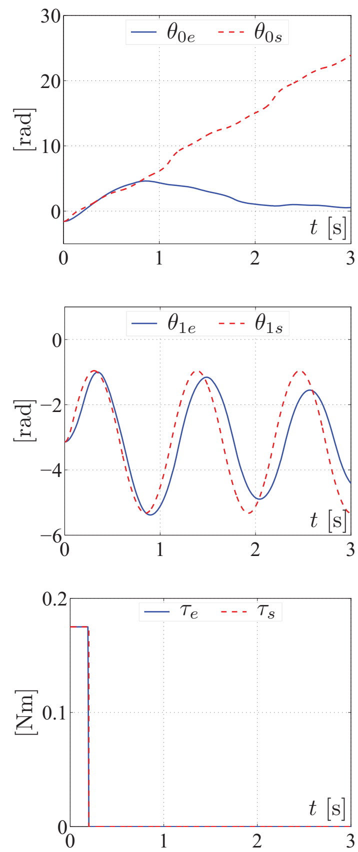


Figure 6. Results.

### B. Discussion

The differences found when comparing the simulation and experimental results (shown in Figure 6) are mainly due to the friction forces, which are not considered in the deduction of the mathematical model associated with (10) and (11). Also, another factor that limits the angular movement of the *arm* in real time experiments, that is $\theta_{0e}$, is the cable of the encoder that senses the variable $\theta_1$, temporarily placed in such a way that offers a minimum resistance to the *arm* movement.

## V. Conclusion

With the intention of providing a useful material for the modeling and construction of a prototype associated with the Furuta pendulum, this paper has presented how to model and build, step-by-step, a Furuta pendulum prototype. Also, numerical simulations of the Furuta pendulum mathematical model, herein deduced, have been performed. Furthermore, experimental tests on the prototype built have been carried out with success, since the obtained results are similar to those predicted by the mathematical model.

Regarding the future work, it would be interesting to consider the dynamics of the actuator and driver in the deduction of the Furuta pendulum mathematical model, herein presented. Some works associated with the dynamics of actuators and drivers are [16]–[19].

## Acknowledgments

The work of M. Antonio-Cruz and C. A. Merlo-Zapata was supported by CONACYT-Mexico and BEIFI scholarships. R. Silva-Ortigoza and M. G. Villarreal-Cervantes acknowledge financial support from Secretaría de Investigación y Posgrado del Instituto Politécnico Nacional (SIP-IPN), SNI-Mexico, and the IPN programs EDI and COFAA. Likewise, the work of D. Muñoz-Carrillo was supported by CONACYT-Mexico scholarship. Lastly, V. M. Hernández-Guzmán acknowledges financial support from SNI-Mexico.

## References

[1] R. Olfati-Saber, "Normal Forms for Underactuated Mechanical Systems With Symmetry," *IEEE Transactions on Automatic Control*, vol. 47, no. 2, pp. 305–308, Feb. 2002.

[2] F. J. Muñoz-Almaraz, E. Freire, and J. Galán-Vioque, "Bifurcation behavior of the Furuta Pendulum," *International Journal of Bifurcation and Chaos*, vol. 17, no. 8, pp. 2571–2578, Aug. 2007.

[3] P. X. La Hera, L. B. Freidovich, A. S. Shiriaev, and U. Mettin, "New approach for swinging up the Furuta Pendulum: Theory and Experiments," *Mechatronics*, vol. 19, pp. 1240–1250, Jul. 2009.

[4] M. Demirtas, Y. Altun, and A. Istanbullu, "Virtual Laboratory for Sliding Mode and PID Control of Rotary Inverted Pendulum," *Computer Applications in Engineering Education*, pp. 400–409, Aug. 2010.

[5] J. Sandoval, R. Kelly, and V. Santibáñez, "Interconnection and damping assignment passivity-based control of a class of underactuated mechanical systems with dynamic friction," *International Journal of Robust and Nonlinear Control*, vol. 21, pp. 738–751, 2011.

[6] P. Seman, B. Rohal'-Ilkiv, M. Juhás, and M. Salaj, "Swinging up the Furuta pendulum and its stabilization via model predictive control," *Journal of Electrical Engineering*, vol. 64, no. 3, pp. 152–158, 2013.

[7] J. Aracil, J. Á. Acosta, and F. Gordillo, "A nonlinear hybrid controller for swinging-up and stabilizing the Furuta pendulum," *Control Engineering Practice*, vol. 21, pp. 989–993, May 2013.

[8] V. M. Hernández-Guzmán, R. Silva-Ortigoza y R. V. Carrillo-Serrano, *Control Automático: Teoría de Diseño, Construcción de Prototipos, Modelado, Identificación y Pruebas Experimentales*, Colección CIDETEC–IPN, Mexico, DF, Mexico: Colección CIDETEC–IPN, 2013, [Online]. Available: http://www.controlautomatico.com.mx

[9] D. Pagano, L. Pizarro, and J. Aracil, "Local bifurcation analysis in the Furuta Pendulum via normal forms," *International Journal of Bifurcation and Chaos*, vol. 10, no. 5, pp. 981–995, May 2000.

[10] J. Á. Acosta, "Furuta's Pendulum: A *Conservative* Nonlinear Model for Theory Validation and Practise," *Mathematical Problems in Engineering*, vol. 2010, pp. 1-29, 2010.

[11] B. S. Cazzolato and Z. Prime, "On the Dynamics of the Furuta Pendulum," *Journal of Control Science and Engineering*, vol. 2011, ID 528341, pp. 8.

[12] S. Jadlovská and J. Sarnovský, "Modelling of classical and rotary inverted pendulum systems–a generalized approach," *Journal of Electrical Engineering*, vol. 64, no. 1, pp. 12–19, 2013.

[13] B. Allota, L. Pugi, and F. Bartolini, "Reinforcement Neural Network for the Stabilization of a Furuta Pendulum," in *Proc. 2nd European Conference on Mechanism Science (EUCOMES)*, Cassino, Italy, Sep. 17–20, 2008, pp. 287–294.

[14] O. García-Alarcón, S, Puga-Guzmán, and J. Moreno-Valenzuela, "On parameter identification of the Furuta pendulum," in *Proc. International Meeting of Electrical Engineering Research (ENIINVIE)*, Ensenada, B. C., Mexico, Mar. 28–30, 2012, pp. 77–84.

[15] C. A. Merlo-Zapata, M. Antonio-Cruz, R. Silva-Ortigoza, H. Taud, I. Rivera-Zárate, D. Muñoz-Carrillo, and V. M. Hernández-Guzmán, "Modeling and Construction of an Inertia Wheel Pendulum Test-bed," *International Conference on Mechatronics, Electronics and Automotive Engineering (ICMEAE)*, Morelos, Mexico, Nov., 2014. Article in Press.

[16] R. Silva-Ortigoza, J. R. García-Sánchez, J. M. Alba-Martínez, V. M. Hernández-Guzmán, M. Marcelino-Aranda, H. Taud, and R. Bautista-Quintero, "Two-Stage control design of a Buck converter/DC motor system without velocity measurements via a $\Sigma - \Delta$-modulator," *Mathematical Problems in Engineering*, vol. 2013, Article ID 929316, pp. 1–11, 2013. [Online]. Available at `http://dx.doi.org/10.1155/2013/929316`

[17] R. Silva-Ortigoza, C. Márquez-Sánchez, F. Carrizosa-Corral, M. Antonio-Cruz, J. M. Alba-Martínez, and G. Saldaña-González "Hierarchical Velocity Control Based on Differential Flatness for a DC/DC Buck Converter–DC Motor System," *Mathematical Problems in Engineering*, vol. 2014, Article ID 912815, pp. 1–12, 2014. [Online]. Available at `http://dx.doi.org/10.1155/2014/912815`

[18] R. Silva-Ortigoza, V. M. Hernández-Guzmán, M. Antonio-Cruz, and D. Muñoz-Carrillo, "DC/DC Buck power converter as a smooth starter for a DC motor based on a hierarchical control," *IEEE Transactions on Power Electronics*. Article in Press. [Online]. Available with DOI: `10.1109/TPEL.2014.2311821`

[19] V. M. Hernández-Guzmán, R. Silva-Ortigoza, and D. Muñoz-Carrillo, "Velocity control of a brushed dc-motor driven by a DC to DC Buck power converter," *International Journal of Innovative Computing, Information and Control*. Article in Press.